Applied Physics B (2022) 128:25
https://doi.org/10.1007/s00340-022-07749-3

Applied Physics B
Lasers and Optics

All-fiber supercontinuum source operating at 1 μm with combination of different PCFs

Huibo Wang[1,2] · Hainian Han[2] · Xiaodong Shao[2] · Ziyue Zhang[2] · Jiangfeng Zhu[1] · Zhiyi Wei[2,3]

Received: 11 June 2021 / Accepted: 3 January 2022

Abstract

We demonstrate an all-fiber scheme for generating supercontinuum spectrum based on a combination method. The configuration employed a nonlinear photonic crystal fiber for dispersion pre-management, an Yb-doped gain fiber for amplification and a special tapered photonic crystal fiber for supercontinuum generation. This setup allows for the generation of highly coherent supercontinuum with 30-dB bandwidth covering from 800 to 1240 nm as well as dispersive waves at 480 nm and 540 nm. The initial pulses were centered at 1030 nm with average power of 90 mW and repetition rate of 216 MHz. Based on the generated supercontinuum and dispersive waves at 540 nm, an envelope-carrier phase offset frequency with signal to noise ratio up to 37 dB was detected by a standard f-2f interferometer. The high signal to noise ratio shows that the infrared supercontinuum and the dispersive waves were highly coherent. Such a robust supercontinuum source achieved at low energy would promote the application of laser comb in precision measurement.

Since the first demonstration of Ti:sapphire laser comb at 2000, optical frequency combs have experienced great development and led to significant advancements in many fields, such as absolute long-distance measurement, exoplanets searching, optical clock and dual-comb spectroscopy [1, 2]. Especially in recent 10 years, with significantly increasing applications in precise metrology, the excellent long-term working performances including high reliability and strong robustness become one of the specific aims for developing more advanced frequency comb technology [3–6]. For this reason, the potential benefits of fiber-laser-based frequency combs, especially all-fiber combs over other combs are obvious. Previous works have shown advantages of the all-fiber combs in terms of stability and long-term operation [7–9]. However, most of all-fiber combs are working in 1.5 μm region and relatively few works have been reported in 1 μm due to the lack of effective method for generating supercontinuum in all-fiber way.

Supercontinuum generation configuration at 1 μm region generally requires bulk grating pairs or chirped mirrors for pulse compression and free-space optical lens with short focus distance for coupling laser pulses into the high nonlinear fibers (HNLF). Such free-space components, however, aggravate instability and complexity in the system, which is an obstacle to mechanical robustness and long-term operation. Therefore, the all-fiber-based supercontinuum generation configuration is urgently desired for building environmentally robust frequency combs. The first key of achieving all-fiber supercontinuum generation is to obtain energetic femtosecond pulses directly from optical fiber without free-space components, which needs precise fiber-based dispersion management. In 1.5 μm region, since the ordinary single-mode fiber introduces anomalous dispersion, the combination of mature dispersion compensation fiber and small-core gain fiber with normal dispersion allows for generating ultrashort pulses in all-fiber-integrated erbium (Er)-doped fiber laser [10–12]. However, for most of Yb-doped ultrafast lasers operating at 1 μm region, achieving fiber-based dispersion management is still a challenge due to the lack of fiber or fiber components with anomalous dispersion. Usual approach for dispersion compensation relies on grating pairs, prisms or chirped mirrors, which increases the vulnerability to environmental disturbance [13]. To achieve

✉ Hainian Han
hnhan@iphy.ac.cn

[1] School of Physics and Optoelectronic Engineering, Xidian University, Xi'an 710071, China

[2] Beijing National Laboratory for Condensed Matter Physics, Institute of Physics, Chinese Academy of Sciences, Beijing 100190, China

[3] School of Physical Sciences, University of Chinese Academy of Science, Beijing 10049, China

Published online: 21 January 2022

pulse compression in all-fiber structure, special fiber and fiber components with anomalous dispersion at 1 μm, such as photonic crystal fiber (PCF) [14], photonic bandgap fiber (PBF) [15, 16], tapered single-mode fiber (TSMF) [17] and chirped fiber Bragg grating (CFBG) [18], are successfully used in Yb-fiber laser for dispersion compensation. Among these components, PCFs with different structures exhibit flexible dispersion, which have proved to be an effective way to compensate the normal dispersion introduced by silica fiber in both intracavity and extracavity [19, 20]. The achievement of anomalous group velocity dispersion (GVD) at near-infrared wavelength in pure silica PCFs results from small mode field area (MFD), which limits the peak power of laser pulse to avoid unnecessary nonlinear effects.

Compact and reliable sub-100 fs Yb-fiber laser operating at 1 μm provides many possibilities for special applications, such as optical frequency combs. Supercontinuum spanning over octave is required for carrier envelope offset (f_{ceo}) detection. However, the limited pulse energy in all-fiber femtosecond operation increases the difficulty of generating over-octave spectrum, which can be overcome by increasing the fiber nonlinearity. One of the effective approaches is to use liquid-core photonic crystal fibers (LC-PCF). By infiltrating the hollow core PCF with various liquids, broadband supercontinuum covering 700–2400 nm was generated in a $C_2H_4Br_2$-filled PCF with pump energy of 0.09 nJ at 1 μm [21]. Benefitting from the high nonlinearity of LC-PCF, the supercontinuum was realized under low pump pulse energy. Tapered photonic crystal fiber is another effective way to achieve high nonlinearity. In 1993, Dumais et al. proposed that the fiber tapering can reduce the effective area and increases the Kerr nonlinear phase shift of the fundamental mode [22]. By heating and stretching ordinary PCF in a flame while ensuring the integrity of the air hole structure, the fiber core diameter can be reduced, while the nonlinearity is improved, which provides convenience for all-fiber supercontinuum generation [23]. The changed MFD of PCF in taper process leads to ZDW shifting, makes it possible to generate dispersive waves with broadband infrared component and visible components under low power injection [24, 25]. Moreover, the tapered fiber can be derived from the commercial fiber, which is easy to obtain and process. Recently, using photonic bandgap fiber and tapered PCF, an all-fiber frequency comb with 22 dB offset frequency was reported in Yb-fiber laser system [26].

In this letter, we present a brief all-fiber way to generate coherent supercontinuum based on a 216 MHz Yb-fiber laser. By employing an anomalous dispersion photonic crystal fiber for dispersion pre-management, laser pulses of 85 fs duration were directly generated from one-stage amplifier without free-space compressor. The supercontinuum and dispersive waves were obtained by injecting amplified pulses into a special designed tapered photonic crystal. Using the obtained supercontinuum, a stable f_{ceo} signal with 37 dB signal to noise ratio and spectrum power stability of 0.08% was detected, which shows the potential of this system to be an ideal spectrum extending apparatus for stable laser frequency combs operating in 1um region.

The schematic diagram of the hybrid all-fiber supercontinuum generation setup is depicted in Fig. 1. The system consisted of a highly integrated fiber oscillator for femtosecond pulses generation, a piece of PCF1 for dispersion management, one-stage Yb-doped fiber amplifier for power boost and a piece of tapered PCF2 for supercontinuum generation. A 216 MHz Yb-doped fiber laser oscillator based on nonlinear polarization rotation was used as seed source in the experiment. The oscillator directly delivered near transform-limited pulses with 100-mW average output power. The measured output spectrum was centered at 1032 nm with 40 nm bandwidth, as shown in Fig. 3a (black curve). At the output end of the oscillator, laser pulses were coupled into single-mode fiber using an aspheric lens. For suppression of acoustic noise and mechanical vibration, fiber laser oscillator together with the following system was packaged in an aluminum box.

In the system, PCF1 (NL-2.3-125-59, YOFC) with length of 2 m was used for pre-dispersion-management. Figure 2 shows the dispersion of PCF1 at different wavelengths while

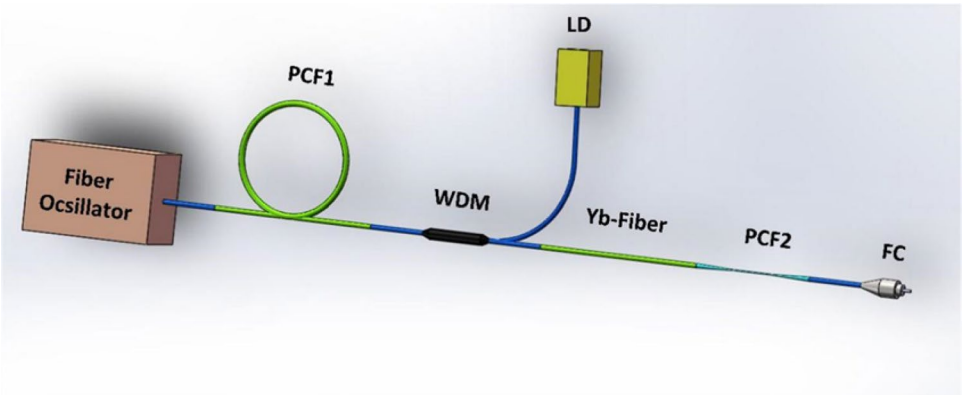

Fig. 1 The schematic diagram of the supercontinuum generation setup. *WDM* wavelength division multiplexer, *LD* laser diode, *FC* optic patch cables

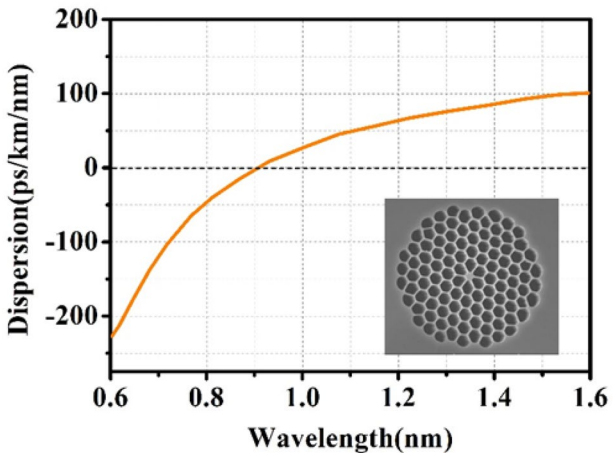

Fig. 2 Dispersion curve of PCF1. Inset: cross-section of PCF1

the inset shows the fiber cross section. The MFD of PCF1 is 2 μm and the ZDW is around 890 nm. Using a commercial simulation software (Rsoft BeamProp), the dispersion parameter of PCF1 was calculated to be 60 ps/nm/km at 1030 nm, which can be used to provide anomalous dispersion in Yb-fiber-based lasers. However, for most of highly nonlinear PCFs, short ZDW usually corresponds to small core diameter and high nonlinearity, which introduce negative influence on laser performance. In the femtosecond domain, dispersive and nonlinear effects dominate the dynamics of pulse propagation. Generally, soliton order N is used as a measure of weight between dispersion and nonlinear effects in nonlinear fiber, which is given by

$$N^2 = \frac{L_D}{L_{NL}} = \frac{\gamma P_0 T_0^2}{|\beta_2|},$$

where L_D is the length of dispersion, L_{NL} is the length of nonlinearity, γ is nonlinear coefficient, P_0 is the peak power of input pulse, T_0 is the pulse width, β_2 is group velocity dispersion [27]. When $N \ll 1$, dispersion plays major role in pulse propagation rather than nonlinearity. In the case of the same fiber used, the way to reduce the value of N is to reduce the power injected into the PCF. On the other hand, because of its relatively small core diameter, PCF1 has a large loss when spliced to a common single-mode fiber. Considerable power would be lost if PCF1 is placed behind the amplifier. To avoid the influence of nonlinearity and the loss of power, PCF1 was placed between the oscillator and the amplifier to pre-compensate the overall system dispersion.

Due to the large difference of the MFD between PCF1 and single-mode fiber, the single-point splice efficiency was about 32%. After two fiber splice processes between SMF and PCF1, the left power injected into the fiber amplifier was only 5 mW. Although most of power was lost during fiber splice processes, it also avoided introducing excessive nonlinearities in the highly nonlinear PCF. The nonlinearity usually leads to changes in frequency distribution. By monitoring the spectrum simultaneously, we confirmed that the spectrum showed no change after passing through PCF1. The autocorrelation trace of the output pulses after PCF1 is shown in Fig. 3b. Assuming a Gaussian shape, the pulse width was 700 fs. It is worth noting that the pulses here contain negative chirp, which can be used to pre-compensate the normal dispersion in amplifier.

After the pre-compensation process, one-stage Yb-doped fiber amplifier with normal dispersion was employed to obtain higher pulse energy with short pulses. The amplifier consisted of 15 cm highly doped Yb-fiber (Yb406, Coractive) for power amplification and a 980/1030 nm WDM for efficient pump light coupling. The output power was 100 mW under 500 mW single-mode pump. After amplifier, the

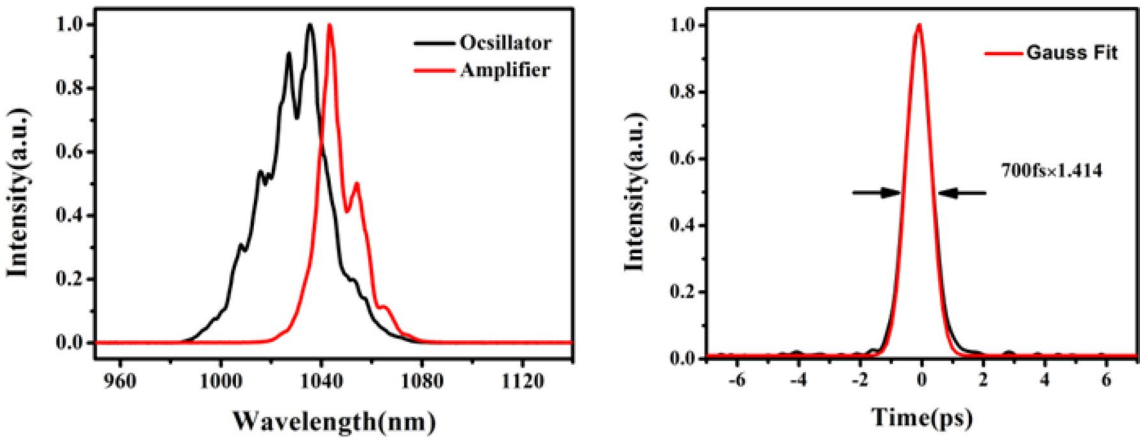

Fig. 3 **a** Experimentally measured output spectrum of oscillator (black) and amplifier (red) in linear scales. **b** Measured autocorrelation traces of the pulses after PCF1

spectrum was red shifted to 1045 nm with bandwidth narrowed to 16 nm, as shown with red curve in Fig. 3a. The corresponding transform-limited pulses duration was 71 fs. In the experiment, the group velocity dispersion (GVD) of Yb-doped fiber and single-mode fiber was 34 fs^2/mm and 23 fs^2/mm at 1 μm, respectively. To compensate the negative chirp and obtain near transform-limited pulses directly from the amplifier, the length of gain fiber and pigtail of WDM were carefully adjusted. Figure 4 shows the measured intensity autocorrelation trace of the amplified pulses. Assuming a $sech^2$-shaped pulse profile, the fitted pulse duration was 83 fs. The pulse duration is also affected by the oscillator. Further output optimization may be possible as the amplified pulse duration is also affected by the spectrum width of the oscillator. Even shorter pulse duration can be obtained by fine-tuning the dispersion of the oscillator.

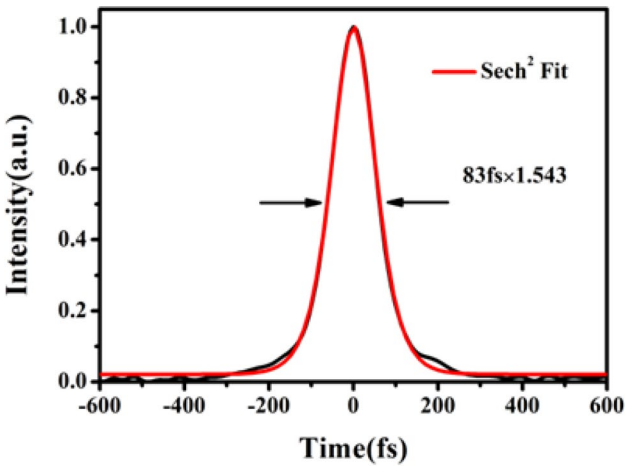

Fig. 4 Autocorrelation trace of the pulses after amplifier

Based on the amplified pulses, we spliced the gain Yb-fiber directly to a segment of tapered PCF (PCF2) for spectrum expansion. The tapered PCF was based on another nonlinear photonic crystal fiber with MFD of 3.6 μm. Fiber with ZDW around 1030 nm was chosen for tapering in order to reduce the influence of the dispersion introduced by untapered section. After tapering, the pitch of fiber was decreased to 2 μm with ZDW blue-shifted. The total length of the tapered fiber was 14 cm with 6-cm taper transition region and 8-cm untapered section for pulse injection. Due to the small difference in MFD of PCF and gain fiber, the fusion efficiency of the two fiber was close to 90%. Figure 5 shows the broadened spectrums from the PCF2 at different input pulse energy. With the increasing of pulse energy, the initial spectrum broadened from the center frequency due to the effect of soliton fission and soliton self-frequency shift. Then, dispersive waves occurred at the short wavelength with high peak intensity around 535 nm, which shows convenience for f_{ceo} detecting. The highly coherent supercontinuum and dispersive waves were collimated by a combination of optical patch cable and aspheric collimator for convenient output.

Since the generated frequency component is closely related to the peak power of the initial pulse, the power and time stability are critical to the frequency distribution in the supercontinuum. Benefit from the all-fiber set up, the ultrafast pulses from the supercontinuum generation configuration showed excellent power stability. Figure 6 (red curve) shows the fluctuation curve of average power after the PCF2 over 12,000 s, corresponding to a root mean square (RMS) value of 0.08%, which illustrates the robustness of the system. For comparison, the power stability of the free-space supercontinuum generation setup using the same seed laser was measured to be 0.31%, as shown in Fig. 6 (gray curve). Furthermore, to investigate the potentiality of this system

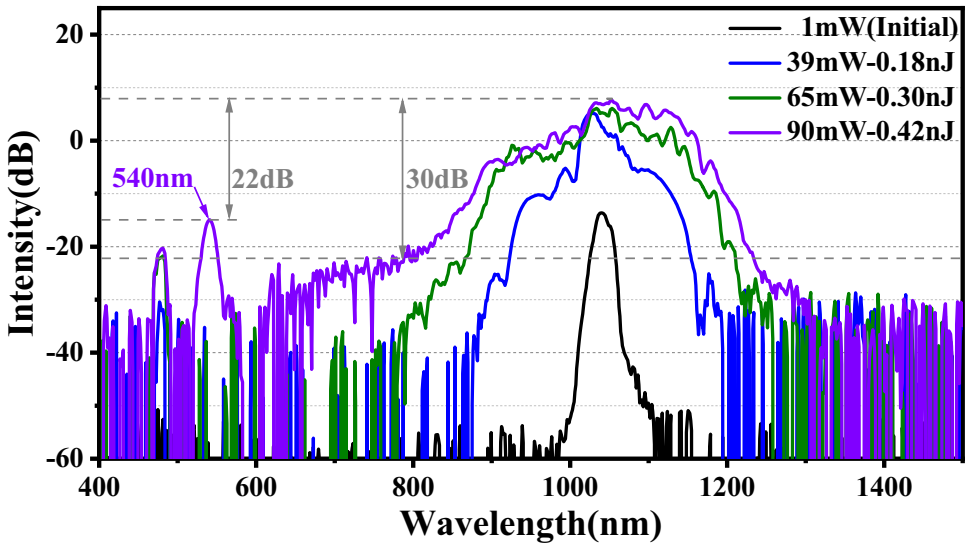

Fig. 5 Dependence of the measured supercontinuum spectrum from PCF2 on the average output power

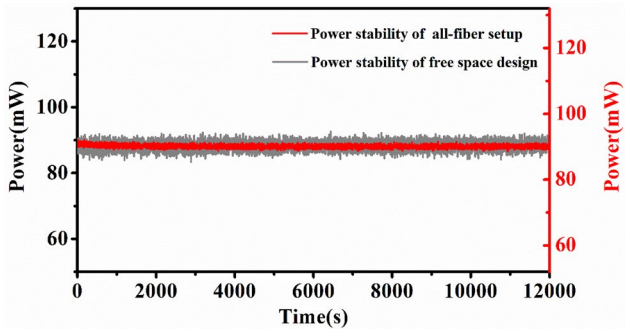

Fig. 6 Stability of all-fiber supercontinuum generation setup (red) and free-space setup (gray)

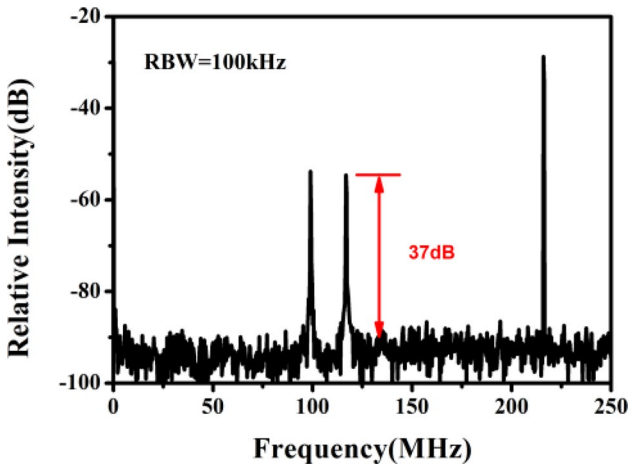

Fig. 7 Detection of free running f_{ceo} signal in a 100 kHz resolution bandwidth

as laser source for fiber frequency comb, a standard f–2f interferometer was built for self-referenced f_{ceo} detection. As shown in Fig. 7, the free-running f_{ceo} with 37 dB signal to noise ratio in a 100 kHz resolution bandwidth was obtained from abovementioned interferometer, which confirmed the high coherence of the supercontinuum and support long-term locking.

We generated a supercontinuum spectrum in an all-fiber 216-MHz Yb-fiber laser. Using 2 m PCF for pre-compressing, 85-fs pulses with 100-mW average output power were directly delivered from the one-stage amplifier. Owing to the short pulses from amplifier, the spectrum expanded a highly coherent supercontinuum with 30-dB bandwidth covering from 800 to 1240 nm with spectrum peaks at 480 nm and 540 nm in a homemade tapered PCF. Based on the detected supercontinuum, a robust 37 dB f_{ceo} signal in a 100 kHz resolution bandwidth and 0.08% supercontinuum light power stability were achieved, which confirmed the superior performance of all-fiber supercontinuum generation design. We believe the all-fiber configuration for supercontinuum generation can be used as an ideal apparatus for frequency combs and may find uses in many laser applications at 1um region.

Acknowledgements The authors would like to thank Yue Meng of YOFC for providing the photonic crystal fiber. The work was supported by the Strategic Priority Research Program of the Chinese Academy of Sciences (Grant Nos. XDA1502040404 and XDB21010400) and the National Natural Science Foundation of China (Grant Nos. 91850209 and 11774234).

Data availability The data that support the findings of this study are available from the corresponding author upon reasonable request.

References

1. T. Udem, R. Holzwarth, T.W. Hänsch, Nature **416**(6877), 233 (2002)
2. A. Apolonski, A. Poppe, G. Tempea, C. Spielmann, T. Udem, R. Holzwarth, T.W. Hänsch, F. Krausz, Phys. Rev. Lett. **85**, 740 (2000)
3. N. Kolachevsky, M. Fischer, S.G. Karshenboim, T.W. Hänsch, Phys. Rev. Lett. **92**(3), 033003 (2004)
4. A.D. Ludlow, T. Zelevinsky, G.K. Campbell, S. Blatt, M.M. Boyd, M.H.G. de Miranda, M.J. Martin, J.W. Thomsen, S.M. Foreman, J. Ye, T.M. Fortier, J.E. Stalnaker, S.A. Diddams, Y. Le Coq, Z.W. Barber, N. Poli, N.D. Lemke, K.M. Beck, C.W. Oates, Science **319**(5871), 1805 (2008)
5. A. Schliesser, N. Picqué, T.W. Hänsch, Nat. Photonics **6**(7), 440 (2012)
6. N. Picqué, T.W. Hänsch, Nat. Photonics **13**(3), 146 (2019)
7. L.C. Sinclair, J.D. Deschênes, L. Sonderhouse, W.C. Swann, I.H. Khader, E. Baumann, N.R. Newbury, I. Coddington, Rev. Sci. Instrum. **86**(8), 081301 (2015)
8. M. Lezius, T. Wilken, C. Deutsch, M. Giunta, O. Mandel, A. Thaller, V. Schkolnik, M. Schiemangk, A. Dinkelaker, A. Kohfeldt, A. Wicht, M. Krutzik, A. Peters, O. Hellmig, H. Duncker, K. Sengstock, P. Windpassinger, K. Lampmann, T. Hülsing, T.W. Hänsch, R. Holzwarth, Optica **3**(12), 1381 (2016)
9. L.C. Sinclair, I. Coddington, W.C. Swann, G.B. Rieker, A. Hati, K. Iwakuni, N.R. Newbury, Opt. Express **22**(6), 6996 (2014)
10. J.W. Nicholson, A.D. Yablon, P.S. Westbrook, K.S. Feder, M.F. Yan, Opt. Express **12**(13), 3025 (2004)
11. B.R. Washburn, S.A. Diddams, N.R. Newbury, J.W. Nicholson, M.F. Yan, C.G. Jorgensen, Opt. Lett. **29**(3), 250 (2004)
12. F. Adler, K.C. Cossel, M.J. Thorpe, I. Hartl, M.E. Fermann, J. Ye, Opt. Lett. **34**(9), 1330 (2009)

13. T. Kurita, H. Yoshida, T. Kawashima, N. Miyanaga, Opt. Lett. **37**(19), 3972 (2012)
14. Z. Zhang, Ç. Şenel, R. Hamid, F.Ö. Ilday, Opt. Lett. **38**(6), 956 (2013)
15. J. Limpert, T. Schreiber, S. Nolte, H. Zellmer, A. Tunnermann, Opt. Express **11**(24), 3332 (2003)
16. H. Lim, F. Wise, Opt. Express **12**(10), 2231 (2004)
17. M. Rusu, R. Herda, S. Kivisto, O.G. Okhotnikov, Opt. Lett. **31**(15), 2257 (2006)
18. S. Kivisto, R. Herda, O.G. Okhotnikov, Opt. Express **16**(1), 265 (2008)
19. H. Lim, F.Ö. Ilday, F.W. Wise, Opt. Express **10**(25), 1497 (2002)
20. B. Xu, A. Martinez, S.Y. Set, S. Yamashita, IEEE Photonics Technol. Lett. **30**(24), 2151 (2018)
21. H.L. Van, V.T. Hoang, T.L. Canh, Q.H. Dinh, H.T. Nguyen, N.V.T. Minh, M. Klimczak, R. Buczynski, R. Kasztelanic, Appl Opt. **60**(24), 7279 (2021)
22. P. Dumais, F. Gonthier, S. Lacroix, J. Bures, A. Villeneuve, P.G.J. Wigley, G.I. Stegeman, Opt. Lett. **18**(23), 1996 (1993)
23. T. Jiang, A. Wang, G. Wang, W. Zhang, F. Niu, C. Li, Z. Zhang, Opt. Express **22**(2), 1835 (2014)
24. I. Cristiani, R. Tediosi, L. Tartara, V. Degiorgio, Opt. Express **12**(1), 124 (2004)
25. H.C. Nguyen, B.T. Kuhlmey, E.C. Mägi, M.J. Steel, P. Domachuk, C.L. Smith, B.J. Eggleton, Appl. Phys. B **81**(2), 377 (2005)
26. Y. Chang, T. Jiang, Z. Zhang, A. Wang, Chin. Opt. Lett. **017**(005), 94 (2019)
27. G.P. Agrawal, *Presented at the nonlinear science at the dawn of the 21st century* (Berlin, 2000)